Vietnam Journal of Earth Sciences, 48(4), 587−608, https://doi.org/10.15625/2615-9783/24948

**Vietnam Journal of Earth Sciences**
https://vjs.ac.vn/index.php/jse



# Soil erosion susceptibility assessment based on the hybrid deep learning models and SHapley analyses

Thuy Ha Thi Nguyen[1], Tuyen Thi Tran[2*], Hieu Ngoc Nguyen[3], Giang Hương Pham[4], Souvik Pal[5], Binh Thai Pham[6]

[1]*School of Agriculture and Resources, Vinh University, Nghe An, Vietnam*
[2]*Faculty of Social Sciences and Arts, Sai Gon University, Ho Chi Minh, Vietnam*
[3]*Nghe An University, Nghe An, Vietnam*
[4]*Thai Nguyen University, Thai Nguyen, Vietnam*
[5]*Department of Computer Science and Engineering, Sister Nivedita University, Kolkata, India*
[6]*Intelligent Geosystems and Infrastructure research group (IGIRG), University of Transport Technology, Hanoi 100000, Vietnam*

Received 20 April 2026; Received in revised form 10 July 2026; Accepted 17 July 2026

ABSTRACT

This study assesses spatial soil erosion susceptibility in Nghe An province, Vietnam, using four novel deep learning models: Deep Neural Network (DNN), Convolutional Neural Network (CNN), Long Short-Term Memory (LSTM), and a hybrid CNN-LSTM architecture. A key innovation of this study is the integration of temporal sequence modeling with spatial feature learning via a hybrid CNN-LSTM architecture, an approach not commonly used in soil erosion studies. In addition, the SHapley Additive exPlanations (SHAP) technique was used to explain how the model worked and how it performed. CNN-LSTM demonstrated the highest validation accuracy (85.7%), sensitivity (0.964), Kappa (0.714), and area under the curve (AUC) of 0.927, along with the lowest error (0.378), outperforming all other models in prediction capability and robustness. While the LSTM model achieved the highest training AUC (0.947) and accuracy (87.7%), it showed signs of overfitting, with a validation accuracy of 83.9%. CNN offered stable performance (validation AUC: 0.892), while DNN lagged, limited by its lack of temporal context (validation AUC: 0.884). Using SHAP, elevation, geology, and aspect were identified as the most critical drivers of erosion susceptibility. The findings underscore the superiority of hybrid deep learning models in capturing the spatiotemporal complexity of erosion processes. The proposed CNN-LSTM model demonstrates strong potential for real-world implementation environments, where both spatial and temporal patterns influence erosion dynamics. This research presents a novel framework for erosion-susceptibility mapping and highlights the importance of integrating interpretable machine learning (via SHAP) with advanced modeling strategies.

*Keywords:* Deep learning, GIS, explainable AI, soil erosion, Vietnam.

## 1. Introduction

Soil erosion is a persistent and pervasive environmental issue that threatens sustainable land management, agricultural productivity, and ecological stability worldwide (Firoozi and Firoozi, 2025). Soil erosion poses a serious environmental threat by diminishing agricultural productivity and vegetation cover. Global soil erosion rates are expected to rise 30% to 66% between 2015 and 2070,

*Corresponding author, Email: tttuyen1982@sgu.edu.vn

depending on different climate and economic scenarios. The problem is particularly acute in regions characterized by heterogeneous topography, variable climatic patterns, and complex land use dynamics (Chakrabortty et al., 2025; Chakrabortty et al., 2020). At present, soil erosion is estimated to reduce worldwide agricultural productivity by approximately $8 billion annually (Sartori et al., 2024). Soil degradation has emerged as a critical issue in densely populated agricultural areas. For example, India supports a large share of the world's population and livestock, but has minimal land resources. This imbalance, worsened by soil degradation, is causing declining crop yields and economic losses, putting food security and farmers' livelihoods at serious risk (Bhattacharyya et al., 2015). In sub-Saharan Africa, soil degradation continues to reduce agricultural productivity and is closely associated with persistent hunger and poverty (Tully et al., 2015). As soils deteriorate, farmers are often compelled to seek out new land for cultivation (Gomiero, 2016). However, most available land in Latin America and Africa consists of marginal areas or tropical forests, which are generally unsuitable for agriculture without substantial investment and improvement (Morgan, 2009). This dynamic underscores the urgent need for sustainable soil management practices to protect existing farmland and prevent further environmental degradation.

Identifying and mapping areas vulnerable to soil erosion is critical for environmental planners aiming to implement effective prevention strategies. Soil erosion susceptibility mapping integrates multiple data sources to highlight regions at risk. Traditional methods of soil erosion assessment, such as those proposed by Renard (1997), while valuable, often fall short in capturing the nonlinear interactions and spatiotemporal complexity inherent in erosion processes. In recent years, machine learning (ML) techniques have revolutionized soil erosion susceptibility mapping. Various ML methods have been applied successfully. For example, Sarkar and Mishra (2018) applied binary logistic regression (BLR) and artificial neural networks (ANN) in India's Purulia district, finding that ANN outperformed BLR. Bag et al. (2022) compared Support Vector Machine (SVM), Classification and Regression Tree (CART), Boosted Regression Tree (BRT), and Random Forest (RF) models, concluding RF performed best. Garrido and Granda (2024) used the LightGBM model in conjunction with the RUSLE model in Ecuador, demonstrating its strong predictive power.

An emerging approach to improving soil erosion assessment involves deep learning (DL) models, computational models inspired by the human brain's neural structure (Saha et al., 2024). These systems are based on ANNs, which simulate the interconnected nature of biological neurons to process complex patterns in data (Ramayanti et al., 2023). DL models have demonstrated exceptional promise across various fields of science due to their ability to extract high-level features from large, complex datasets. The published literature consists of numerous review articles that lay the groundwork for understanding DL. Notably, LeCun et al. (2015), Bengio et al. (2021), and Janiesch et al. (2021) introduced the core principles and essential components. In addition, comprehensive surveys, such as those by Matsuo et al. (2022), explored foundational DL models, including convolutional neural networks (CNNs) and recurrent neural networks (RNNs). More recent reviews have shifted focus toward domain-specific advancements, highlighting DL applications in areas such as healthcare (Abdel-Jaber et al., 2022), finance (Ozbayoglu et al., 2020), image processing (Archana and Jeevaraj, 2024), and environmental research (Zhang et al., 2022).

Despite this growing body of literature, DL models have been used relatively sparingly in soil erosion studies. This study aims to address this gap by conducting a comprehensive comparison of four state-of-the-art deep learning architectures, i.e., CNN, Deep Neural Network (DNN), Long Short-Term Memory (LSTM), and a hybrid CNN-LSTM model, for soil erosion susceptibility mapping in Nghe An province. By incorporating ten critical environmental and topographic variables, our study explores how different model architectures handle spatial features and their interaction in erosion prediction. A key innovation in our study is the application of a hybrid CNN-LSTM model, which uniquely combines the spatial learning strengths of CNNs with the sequential pattern-recognition capabilities of LSTMs. To further enhance model interpretability, we employed SHapley Additive exPlanations (SHAP) to identify and rank the most influential predictors of erosion. Through rigorous model evaluation using multiple performance metrics, our study not only advances the methodological framework for erosion susceptibility mapping but also provides actionable insights for land management in data-rich environments.

## 2. Description of the study area

The study was conducted in Nghe An Province, located in the North Central Coast region of Vietnam. The province extends approximately from 18°33' to 20°00'N and from 103°52' to 105°48'E, bordering Laos to the west, Thanh Hoa Province to the north, Ha Tinh Province to the south, and the East Sea to the east (Fig. 1). Nghe An encompasses diverse topography, from coastal plains to extensive mountainous landscapes. The western part of the province belongs to the northern Truong Son Mountain Range and is characterized by rugged terrain, steep slopes, deeply incised valleys, and dense drainage networks.

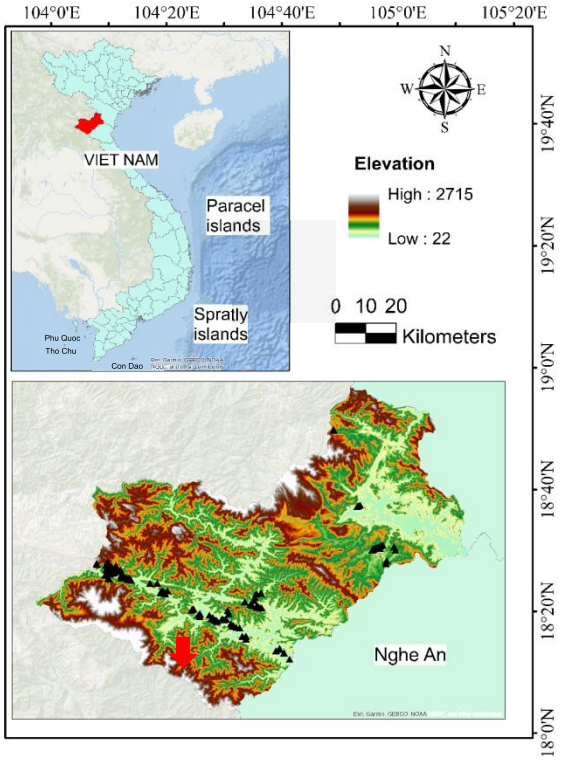



*Figure 1.* Location map of the study area and historical soil erosions

This study focuses on the mountainous districts of western Nghe An, where settlements are primarily concentrated along river valleys and lower slope areas. The region experiences a tropical monsoon climate with pronounced wet and dry seasons. Annual rainfall is highly seasonal, concentrated between August and November, when tropical storms, typhoons, and associated extreme rainfall events frequently affect Central Vietnam. The combination of intense precipitation, steep topography, weathered geological formations, and dense river systems creates favorable conditions for soil erosion.

## 3. Data and methods

### *3.1. Data*

#### *3.1.1. Soil erosion inventory*

Areas affected by soil erosion within the study area were identified through a combination of documentary review, interpretation of Google Earth and satellite imagery, and field surveys supported by GPS observations. To reduce the potential effects of spatial autocorrelation and avoid spatial dependence among samples, the identified erosion locations were subjected to a spatial thinning procedure during data preprocessing using GIS tools, retaining only one erosion point per mapping pixel/resolution unit (Jaafari et al., 2026; Pham et al., 2026). After this filtering process, a total of 119 spatially independent soil erosion locations were retained for analysis (Fig. 1). These samples were then randomly divided into training (70%) and validation (30%) datasets for model development and evaluation (Pham et al. 2020; Adnan et al. 2021).

#### *3.1.2. Soil erosion influencing factors*

In this study, eleven critical geoenvironmental factors were integrated into the soil erosion modeling framework. These factors include elevation, slope, aspect, curvature, flow accumulation, stream power index (SPI), topographic wetness index (TWI), normalized difference vegetation index (NDVI), geology, soil type, and rainfall (Fig. 2). Topographic attributes such as elevation, slope, aspect, curvature, flow accumulation, SPI, and TWI were derived from a 30 m resolution Digital Elevation Model (DEM) obtained from the Advanced Spaceborne Thermal Emission and Reflection Radiometer (ASTER) database. The NDVI layer was generated using Landsat 7 satellite imagery provided by the United States Geological Survey (USGS). In contrast, geological, soil, and rainfall data were gathered from a combination of existing literature, thematic maps, and datasets produced by recognized government and scientific institutions.

Each factor plays a unique and influential role in determining the spatial patterns and severity of soil erosion. Collectively, these variables provide a robust foundation for spatially explicit soil erosion modeling, enabling better risk assessment, land management planning, and implementation of erosion control measures. A detailed discussion of the significance of each variable in relation to erosion processes is provided below:

Elevation is a primary determinant of climatic conditions, such as temperature and precipitation, which, in turn, influence vegetation patterns, soil formation, and erosion susceptibility (Thanh et al. 2020). Higher elevations are often associated with cooler temperatures and increased precipitation, potentially accelerating erosion due to snowmelt and heavy rainfall (Podhrázská et al. 2025). Moreover, elevation affects the types and distribution of vegetation, which can either protect or expose the soil surface to erosive forces (Nahib et al. 2024).

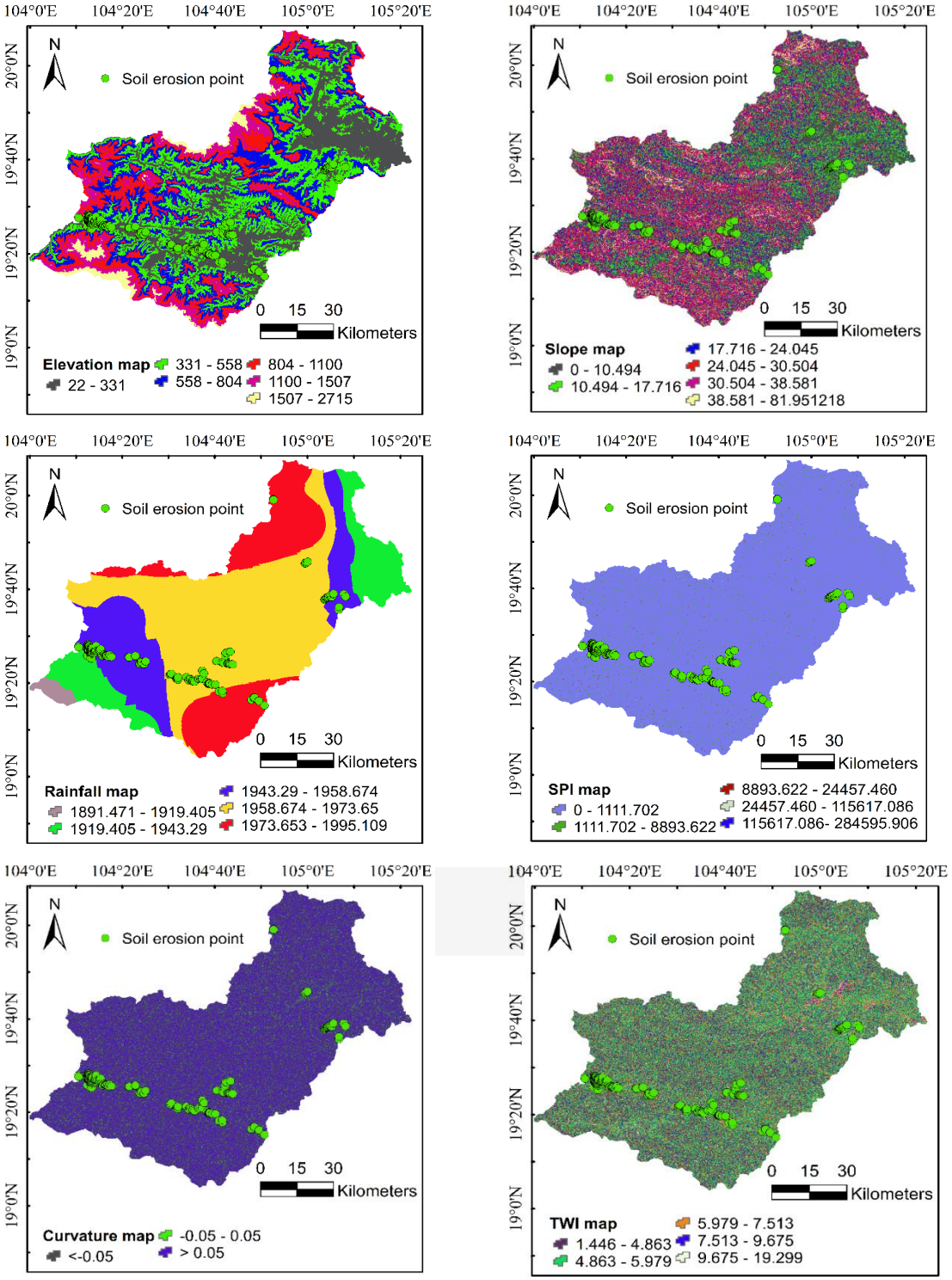



*Figure 2*. Thematic maps of the factors used in this study

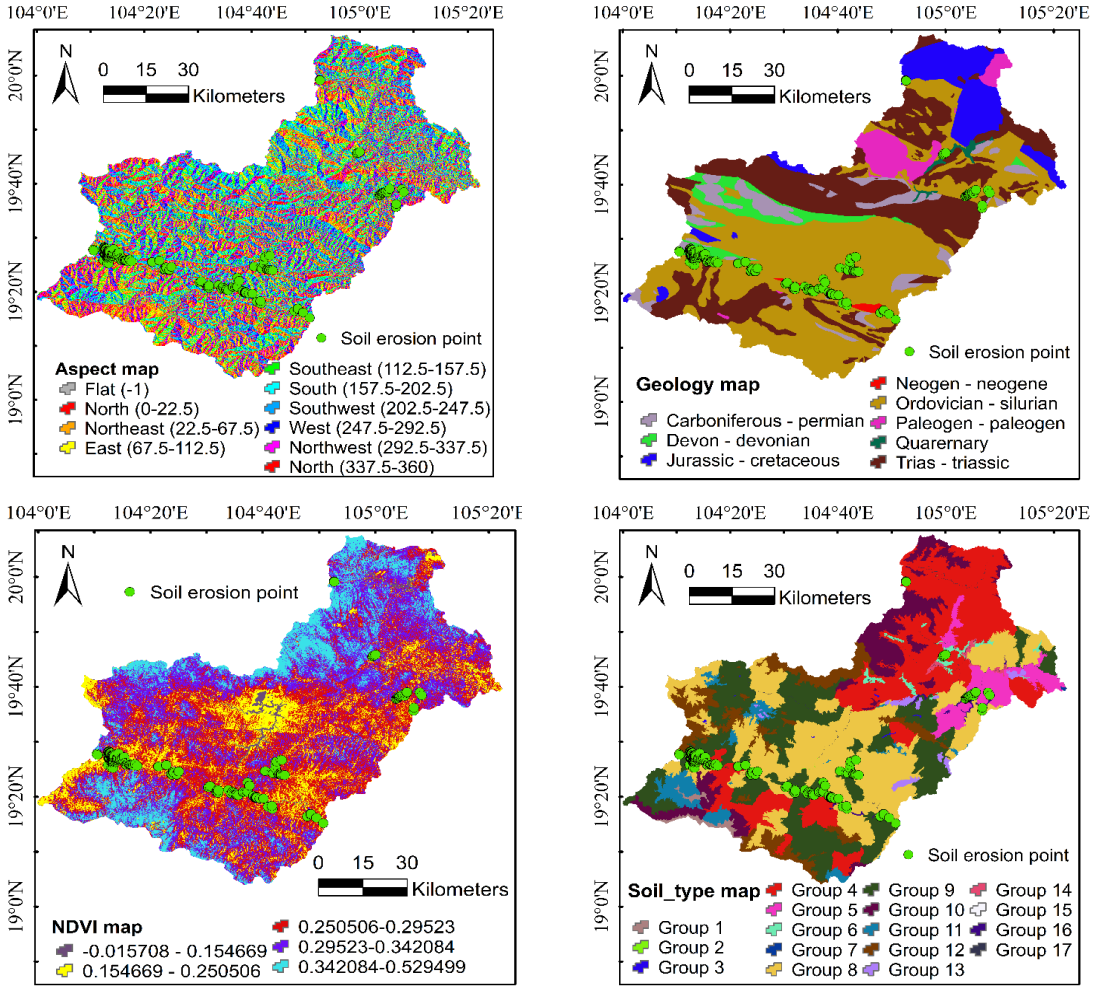



*Figure 2*. Cont.

Aspect, or the orientation of a slope, controls exposure to solar radiation and prevailing winds. Slopes facing south (in the Northern Hemisphere) typically receive more sunlight, leading to drier conditions and sparse vegetation, thereby increasing erosion vulnerability (Huntley, 2023). On the other hand, north-facing slopes tend to retain moisture and support denser vegetation, which can reduce erosion by shielding the soil from raindrop impact and surface runoff (Pelletier et al., 2018).

Slope gradient plays a vital role in the speed and volume of water movement across the land surface (Tran et al., 2020). Steeper slopes facilitate faster runoff, enhancing the erosive power of flowing water and increasing the potential for detaching and transporting soil particles downslope (Yousefi et al., 2022). In contrast, gentle slopes allow more time for infiltration and less momentum for erosion, making them relatively more stable.

Curvature describes the convexity or concavity of the terrain (Kennelly, 2008). Concave surfaces, such as valleys or depressions, tend to concentrate water flow, increasing the potential for localized erosion by intensifying hydraulic forces (Gabbard et

al., 1998). Convex surfaces, such as ridges, promote water dispersion, which can reduce erosion risk by limiting concentrated flow (Rieke-Zapp and Nearing, 2005).

Flow accumulation quantifies the number of upstream cells draining into a specific point, indicating potential water pathways and convergence zones (Kader et al., 2024). High flow accumulation values typically signify areas of concentrated runoff, which are more likely to become channels and gullies prone to severe erosion.

SPI is a compound indicator that combines slope and flow accumulation to estimate the erosive energy exerted by surface runoff (Singh et al., 2025). Areas with high SPI values are more likely to experience intense erosion due to the high kinetic energy of concentrated, fast-moving water (Tran et al., 2020). This index is particularly useful in identifying potential headwater erosion zones and riverbank instability.

TWI represents the spatial distribution of soil moisture as a function of local upslope contributing area and slope (Kopecký et al., 2021). High TWI values indicate zones with higher moisture retention, often associated with saturation and reduced soil shear strength. Such areas are more prone to erosion, especially under prolonged wet conditions or after heavy rainfall events (Istanbulluoglu and Bras, 2005, 2006).

NDVI serves as a proxy for vegetation health and density. Vegetation plays a protective role in soil conservation by reducing the impact of raindrops, minimizing runoff velocity, and anchoring soil with root systems (Zuazo and Pleguezuelo, 2009). Higher NDVI values typically indicate areas with dense vegetation cover, which are less susceptible to erosion, whereas lower NDVI values suggest barren or sparsely vegetated areas more prone to degradation (Istanbulluoglu and Bras, 2005, 2006).

Geology influences erosion through the type and resistance of the underlying rock formations. Soft sedimentary rocks like shale and sandstone erode more rapidly than igneous or metamorphic rocks such as granite or basalt. Rock structure, stratification, and fracturing also affect how easily soil and rock materials are detached and transported by erosive forces (Flowers and Ehlers, 2018).

Soil type affects erosion through physical and chemical properties such as texture, cohesion, permeability, and organic matter content. Sandy soils, due to their coarse texture and low cohesion, are highly prone to erosion. In contrast, clayey soils may resist erosion better due to higher cohesion but can still erode significantly under intense rainfall if surface crusting or compaction occurs (Garrido and Granda, 2024; Jaafari et al., 2015).

Rainfall is a major external driver of erosion. Both rainfall intensity and duration influence the detachment of soil particles and the formation of overland flow (Kinnell, 2005). High-intensity rainfall can exceed the soil's infiltration capacity, leading to surface runoff that carries soil particles downhill (Tarboton, 2003). Seasonal variations in rainfall also play a crucial role in temporal erosion dynamics (Mosaffaie et al., 2015).

When assessing soil erosion susceptibility, it is essential to identify and remove highly correlated variables, as their presence can skew model outcomes. Although deep learning models are generally capable of handling multicollinearity, VIF-based filtering was applied in this study as a precautionary step to reduce feature redundancy and improve the clarity of SHAP-based interpretation. Highly correlated predictors may distribute importance across multiple variables, making it more difficult to distinguish the individual contribution of each factor. Therefore, feature parsimony was prioritized to enhance model interpretability. Two widely used methods for this task are Pearson's correlation coefficient (r) and variance inflation factor (VIF). Pearson's r

quantifies the strength and direction of their relationships, while VIF helps identify multicollinearity among variables. According to recommendations given in the literature (Jaafari et al. 2022), any variable with a Pearson's r above 0.7 or a VIF greater than 5 should be excluded from the analysis. The correlation analysis indicated a strong association between the flow accumulation and SPI (Fig. 3). Table 1 displays the VIF values calculated for the variables in this study, all of which were below 3, suggesting minimal multicollinearity. Since flow accumulation had the highest VIF among the variables (2.74), it was removed from further analysis to avoid bias or errors in the modeling process.

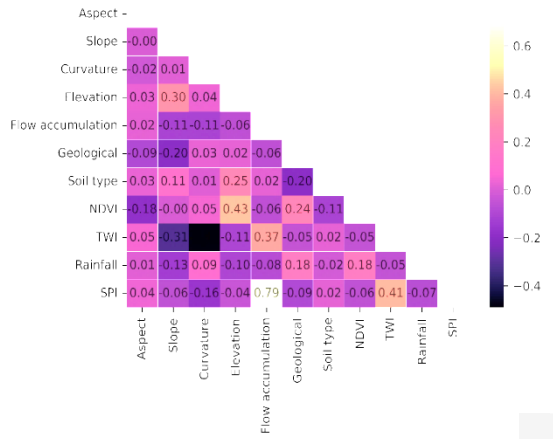



*Figure 3.* Correlation matrix of the influencing factors

*Table 1.* Variance inflation factor (VIF) of the influencing factors

| No. | Variable | VIF |
|---|---|---|
| 1 | Aspect | 1.066 |
| 2 | Slope | 1.342 |
| 3 | Curvature | 1.371 |
| 4 | Elevation | 1.619 |
| 5 | Geological | 1.173 |
| 6 | Flow accumulation | 2.740 |
| 7 | Soil type | 1.181 |
| 8 | NDVI | 1.529 |
| 9 | TWI | 1.786 |
| 10 | Rainfall | 1.130 |
| 11 | SPI | 1.219 |

### *3.2. Methods*

#### *3.2.1. Deep Neural Network (DNN)*

DNN is a type of artificial neural network characterized by multiple layers of interconnected nodes, or neurons, between the input and output layers (Schmidhuber, 2015). These hidden layers enable the network to learn complex, abstract representations of data by transforming the input through successive nonlinear transformations (Dao et al., 2020). Each neuron in a DNN receives inputs, applies a weighted sum, passes it through an activation function (such as ReLU, sigmoid, or tanh), and forwards the result to the next layer. During training, the network adjusts the weights of these connections using backpropagation, which minimizes the error between predicted and actual outputs via optimization algorithms such as stochastic gradient descent. DNNs are versatile and can be used for various tasks, including image and speech recognition, natural language processing, fraud detection, and recommendation systems, as well as natural hazards modeling (Van Phong et al., 2025; Panahi et al., 2021; Dao et al., 2020; Ghasemian et al., 2022).

#### *3.2.2. Convolutional Neural Network (CNN)*

Among the various types of DLAs, CNNs have emerged as one of the most influential and widely used architectures (Yamashita et al., 2018; Kumar et al., 2025). Initially introduced by CNNs, they are increasingly applied in geosciences for satellite imagery classification and natural hazard susceptibility mapping (Ma and Mei, 2021). Their primary advantage is the ability to automatically learn spatial hierarchies of features, making them ideal for geospatial pattern analysis (Maxwell et al., 2023). The architecture comprises hierarchical layers, local receptive fields, and shared weights. Central to the design are convolutional layers, which apply filters to detect local features, and pooling layers,

which reduce spatial dimensionality to lower computational load and mitigate overfitting (Razi et al., 2023). Nonlinear activation functions, such as the Rectified Linear Unit (ReLU), allow the network to model complex representations. Various specialized architectures, including GoogleNet, ZFNet, and VGGNet, have been developed to optimize depth and connectivity for specific tasks (Panahi et al., 2021). This structural versatility ensures that CNNs remain a robust choice for modeling complex environmental dependencies.

*3.2.3. Long Short-Term Memory (LSTM)*

LSTM networks are a specialized architecture of Recurrent Neural Networks (RNNs) engineered to capture long-range dependencies in sequential data while mitigating the vanishing gradient problem (Hochreiter and Schmidhuber, 1997; Nguyen et al., 2023). Unlike standard RNNs, LSTMs utilize a sophisticated internal structure to retain information over extended intervals (Ewees et al., 2022). The core of an LSTM unit is the memory cell, which serves as a state reservoir modulated by three essential gates: the input gate ($i_t$), forget gate ($f_t$), and output gate ($o_t$). These gates collectively regulate the information flow ($x_t$) into and out of the cell (Ehteram et al., 2024; Hochreiter and Schmidhuber). The process operates iteratively at each time step, utilizing the current input vector and the previous hidden state to update the network (Pentsos et al., 2025). The forget gate determines which portions of the previous state to discard to prevent the accumulation of irrelevant data, while the input gate identifies which new information to store (Singh et al., 2025). Simultaneously, candidate values are generated and filtered before the cell state is updated. Finally, the output gate decides which information from the updated cell state to expose as the hidden state, which serves as a summary of the sequence context (Fathalla et al., 2022; Malashin et al., 2024). This mechanism allows the LSTM to adaptively maintain memory over time, making it highly effective for complex sequence prediction tasks in environmental and geomorphological modeling (Mienye et al., 2024).

*3.2.4. Hybrid CNN-LSTM model*

A hybrid CNN-LSTM model combines the strengths of CNNs in spatial feature extraction with the capabilities of LSTMs in modeling temporal or sequential dependencies. This architecture is particularly well-suited for complex environmental modeling tasks such as soil erosion susceptibility assessment, where both spatial and temporal factors play critical roles. In this hybrid model, the CNN component serves as the front-end processor, extracting high-level spatial features from input datasets, such as satellite imagery, DEMs, land-use and land-cover maps, and soil property grids. These convolutional layers are adept at detecting spatial patterns and local dependencies related to terrain attributes, vegetation cover, and rainfall distribution, factors that are crucial for understanding the spatial variability of soil erosion. Once spatial features are extracted, they are reshaped into a sequential format and passed to the LSTM layers. The LSTM component models the temporal dynamics of soil erosion processes. Soil erosion is not only influenced by static factors but also by dynamic, time-dependent variables such as seasonal rainfall, antecedent soil moisture conditions, and changes in vegetation cover. The LSTM layers process sequences of such data, enabling the model to account for long-term dependencies and historical influences, which are often essential for accurately predicting erosion susceptibility. Following the LSTM processing, the output is passed through fully connected layers to generate the final prediction, which may be expressed as a

susceptibility score or classified into risk categories for each spatial unit (e.g., pixel or grid cell). This architecture effectively integrates spatial and temporal features, allowing for a comprehensive understanding of the erosion process. The CNN-LSTM model is particularly justified for soil erosion modeling because it captures the complex, nonlinear interactions among multiple environmental variables. Soil erosion results from the interplay of various factors such as slope gradient, rainfall intensity, soil type, and land management practices. The CNN-LSTM architecture can learn these relationships directly from data, eliminating the need for predefined equations or manual feature engineering. Moreover, the model's ability to handle both spatial heterogeneity and temporal variation improves its generalization across different geographic regions and climatic conditions. It can also work efficiently in settings where spatial data is abundant but temporal data is limited, leveraging CNN-extracted features while still benefiting from LSTM's temporal learning. By modeling both where and when erosion is likely to occur, the CNN-LSTM hybrid model provides a robust, data-driven approach for soil erosion susceptibility mapping.

*3.2.5. Validation metrics*

In this study, a range of validation metrics was used to comprehensively evaluate model performance. These include classification performance measures derived from the confusion matrix: True Positives (TP), True Negatives (TN), False Positives (FP), and False Negatives (FN). Based on these values, we calculated the Positive Predictive Value (PPV), Negative Predictive Value (NPV), Sensitivity (SST), Specificity (SPF), and Overall Accuracy (ACC). Additionally, the Cohen's Kappa coefficient was employed to evaluate classification robustness. At the same time, Mean Absolute Error (MAE) and Root Mean Squared Error (RMSE) were used to quantify the magnitude of prediction errors (Nguyen et al., 2025; Nhat et al., 2025). Finally, the area under the Receiver Operating Characteristic Curve (AUC) was utilized as the primary indicator of the models' discriminative capability (Le Minh et al., 2023; Pham et al., 2026; Doan et al., 2026; Kumar et al., 2026; Dinh et al., 2026; Nguyen et al., 2026; Hieu et al., 2026).

*3.2.6. SHapley Additive exPlanations (SHAP)*

SHAP is a powerful and widely adopted method for interpreting machine learning models by attributing a model's output to its input features (Lundberg and Lee, 2017). Rooted in cooperative game theory, SHAP uses Shapley values to fairly and consistently distribute a model's prediction across its features. Each feature is treated as a player in a game where the goal is to explain the model's output, and the Shapley value quantifies each feature's contribution to that prediction. One of SHA-P's most important characteristics is its additive nature, meaning it breaks down a model's output into a sum of individual feature contributions. It is model-agnostic, making it applicable to any machine learning model, including linear regression, decision trees, ensembles, and neural networks (Yousefi et al., 2026; Choubin et al., 2025). This generality enables SHAP to serve as a unified framework for interpreting complex models in a transparent and theoretically sound manner. To compute Shapley values in practice, SHAP examines feature combinations (or coalitions) by systematically permuting them across instances in the dataset. For each feature, SHAP calculates the change in the model's output when that feature is added to a subset of the other features. These marginal contributions are then averaged across all possible subsets to yield the final Shapley value.

## 4. Modeling environment

To perform the model, we used TensorFlow with Keras in Python, employing its high-level abstraction and modular design to streamline the development of deep learning architectures. The Sequential API was employed to construct and organize the layers of each model, enabling rapid prototyping and clear model definition (Table 2). Data preprocessing was conducted before model training, including normalization and reshaping, as needed, particularly for CNN and LSTM inputs. The training process was managed using the fit() function, which facilitated the integration of callbacks such as early stopping. This mechanism monitored validation loss and halted training when performance plateaued, thereby mitigating overfitting and reducing unnecessary computation. ReLU was adopted as the primary activation function because of its computational efficiency and fast convergence during deep network training. To mitigate potential issues such as dying ReLU units and gradient sparsity, He initialization was applied to the network weights, and Batch Normalization layers were incorporated into the CNN and DNN architectures to maintain stable activation distributions during training. Model evaluation was performed using standard metrics described in Subsection 3.2.5, with validation data split from the training set to assess generalization.

*Table 2.* Configuration of the DNN, CNN, and LSTM models

| Parameter | DNN | CNN | LSTM |
|---|---|---|---|
| No. of layers | 7 | 7 | 3 |
| Activation function | ReLU | ReLU | Sigmoid |
| Dropout | 0.2 | 0.5 | - |
| Optimizer | Adam (Adaptive Moment Estimation) | Adam (Adaptive Moment Estimation) | Adam (Adaptive Moment Estimation) |
| Learning rate | 0.001 | 0.001 | 0.001 |
| Epochs | 500 | 500 | 500 |
| Loss function | binary_crossentropy | binary_crossentropy | binary_crossentropy |
| Early stopping | Yes | Yes | Yes |

## 5. Results

### *5.1. Validation and comparison of the models*

During the training phase (Table 3), the performance of four models was evaluated using several key metrics. The LSTM model demonstrated the strongest overall performance, achieving the highest sensitivity (SST = 91.2%), accuracy (ACC = 87.7%), and Kappa coefficient (Kappa = 0.755), along with the lowest error rates (MAE = 0.123 and RMSE = 0.35). LSTM also showed strong specificity (SPF = 84.3%), indicating effective classification with a good balance between true and false positives. The CNN-LSTM hybrid model followed closely, particularly excelling in negative predictive value (NPV = 94.8%) and showing competitive accuracy (84.5%) and Kappa (0.691), suggesting its strength in minimizing false negatives. The DNN model performed moderately well, with reasonable sensitivity (88.4%) and accuracy (83%), but lagged in specificity (77.7%) and showed higher error (RMSE = 0.412). Lastly, the CNN model demonstrated solid performance with balanced metrics, though it underperformed the LSTM model in terms of sensitivity (83%) and Kappa (0.655), despite comparable positive predictive value (PPV = 82.4%). Overall, the LSTM model outperformed the others during training, demonstrating superior learning capability and generalization, followed by CNN-LSTM, DNN, and CNN in descending order.

During the validation phase (Table 3), the LSTM model continued to perform well,

achieving the highest accuracy (ACC = 83.9%) and Kappa coefficient (K = 0.678) among all models. This model also showed a strong negative predictive value (NPV = 85.1%), indicating its effectiveness in correctly identifying true negatives. However, compared with training, its specificity (SPF = 82%) decreased slightly, suggesting a slight increase in false positives. The CNN-LSTM hybrid model emerged as the best-performing model in validation, particularly in terms of accuracy (ACC = 85.7%) and Kappa (K = 0.714), surpassing other models. The hybrid model also demonstrated the highest NPV (95.4%), confirming its robustness in minimizing false negatives and providing reliable predictions for negative instances. The DNN model maintained stable performance with an accuracy of 85.4% and a Kappa of 0.708, showing good generalization to unseen data. The model outperformed CNN in most metrics and maintained a higher specificity (80.8%) than CNN and LSTM. The CNN model performed reasonably well but ranked last in several key measures, including sensitivity (SST = 82.6%) and Kappa (K = 0.678). Its positive predictive value (PPV = 83.7%) was strong, indicating reliable positive classifications, though it lagged behind others in overall balance and consistency. Overall, the hybrid CNN-LSTM model achieved the best validation performance, followed closely by DNN and LSTM, while CNN performed comparatively worse.

*Table 3.* Performance analysis of the models

| No. | Metric | Training phase | | | | Validation phase | | | |
|---|---|---|---|---|---|---|---|---|---|
| | | CNN | LSTM | DNN | CNN-LSTM | CNN | LSTM | DNN | CNN-LSTM |
| 1 | TP | 322 | 354 | 343 | 368 | 149 | 145 | 152 | 163 |
| 2 | TN | 326 | 333 | 307 | 294 | 138 | 137 | 135 | 125 |
| 3 | FP | 69 | 62 | 88 | 101 | 29 | 30 | 32 | 42 |
| 4 | FN | 66 | 34 | 45 | 20 | 20 | 24 | 17 | 6 |
| 5 | PPV | 0.824 | 0.851 | 0.796 | 0.785 | 0.837 | 0.829 | 0.826 | 0.795 |
| 6 | NPV | 0.832 | 0.907 | 0.872 | 0.936 | 0.873 | 0.851 | 0.888 | 0.954 |
| 7 | SST | 0.83 | 0.912 | 0.884 | 0.948 | 0.882 | 0.858 | 0.899 | 0.964 |
| 8 | SPF | 0.825 | 0.843 | 0.777 | 0.744 | 0.826 | 0.82 | 0.808 | 0.749 |
| 9 | ACC | 0.828 | 0.877 | 0.83 | 0.845 | 0.854 | 0.839 | 0.854 | 0.857 |
| 10 | Kappa | 0.655 | 0.755 | 0.661 | 0.691 | 0.708 | 0.678 | 0.708 | 0.714 |
| 11 | MAE | 0.172 | 0.123 | 0.17 | 0.155 | 0.146 | 0.161 | 0.146 | 0.143 |
| 12 | RMSE | 0.415 | 0.35 | 0.412 | 0.393 | 0.382 | 0.401 | 0.382 | 0.378 |

A comparison of model performance across training and validation phases shows that LSTM performed best during training but showed slight overfitting in validation. CNN-LSTM improved in validation, achieving the highest validation accuracy and Kappa, demonstrating excellent generalization. DNN remained stable, with consistent results across both phases, while CNN underperformed in both phases. Although LSTM performed well during training, the hybrid CNN-LSTM proved most reliable for real-world applications, with minimal performance drop and superior validation metrics, making it the preferred model overall.

To further evaluate and compare model performance across both phases, we employed the widely accepted AUC metric. During the training phase (Fig. 4), the LSTM model achieved the highest AUC of 0.947, demonstrating outstanding discriminative capability. The CNN-LSTM model performed closely, with an AUC of 0.929, while the CNN and DNN models recorded slightly lower AUCs of 0.896 and 0.884, respectively. In the validation phase (Fig. 5), the LSTM model maintained a high AUC of 0.919, whereas the CNN-LSTM model showed a slight improvement, achieving an AUC of 0.927 and outperforming the LSTM. The

CNN and DNN models remained consistent, with AUCs of 0.892 and 0.884, respectively. These results indicate that both the LSTM and CNN-LSTM models generalize effectively to unseen data, with the hybrid CNN-LSTM model demonstrating slightly superior robustness and adaptability in real-world scenarios.

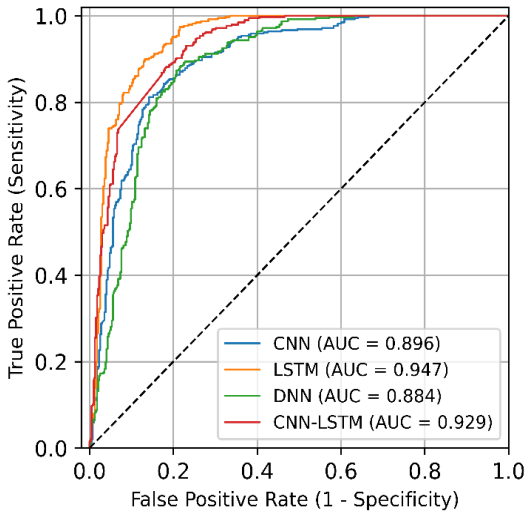



*Figure 4.* AUC values of the models in the training phase

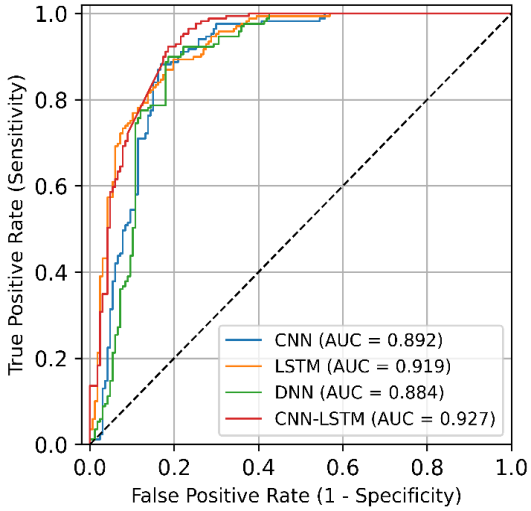



*Figure 5.* AUC values of the models in the validation phase

### *5.2. Key driving factors*

Figure 6 presents a SHAP summary plot showing the relative influence of each soil erosion factor on the hybrid CNN-LSTM model's predictions. In this plot, SHAP values quantify the contribution of influencing factors to the model's output for each data instance, with positive values indicating a factor's role in increasing the predicted outcome and negative values indicating a decreasing effect. Among the evaluated variables, geology and elevation emerged as the most influential drivers, with SHAP values of 0.14. This is evidenced by the broad distribution of their SHAP values along the x-axis, signifying a strong and variable impact on model predictions. The spread of SHAP values for these variables indicates that different geological and elevation classes can either increase or decrease the predicted risk of soil erosion. Both high and low variables' values (as indicated by the color gradient) are associated with a range of positive and negative impacts, underscoring the importance of underlying geology and elevation in determining soil erosion susceptibility. Aspect (0.12) also exhibited considerable influence, with a substantial spread of SHAP values. This suggests that variations in aspect can substantially affect model predictions, likely because they influence water flow, runoff, and exposure. Slope (0.04) and soil type (0.03) had moderate importance, with SHAP values that are more concentrated near zero but still display some spread. This indicates that while these variables contribute to the model, their impact is less pronounced than that of geological, elevation, and aspect variables. In contrast, rainfall (0.02), NDVI (0.02), curvature (0.01), and TWI (0.01) had a limited impact on the model, indicated by SHAP values tightly clustered around zero. Among all variables, SPI contributed almost nothing, with SHAP values essentially zero, making it the least impactful feature in this analysis.

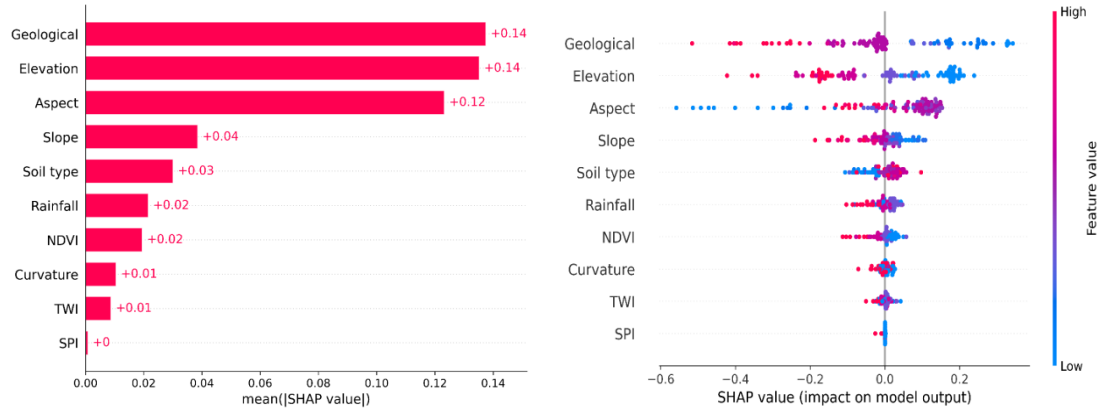



*Figure 6*. SHAP summary plots showing each variable's influence on the hybrid CNN-LSTM model predictions

### *5.3. Soil erosion susceptibility map*

A soil erosion susceptibility map for the study area was generated using the hybrid CNN-LSTM model (Fig. 7). This model classified the region into five susceptibility categories: very low, low, moderate, high, and very high, which accounted for 60.9%, 6.7%, 6%, 19.6%, and 6.8% of the total area, respectively (Fig. 8 - blue line and values). Analysis of the proportion of erosion-affected pixels demonstrated a strong alignment between the model's susceptibility classes and the actual distribution of erosion occurrences (Fig. 8 - red line and values). Notably, 0.7% of all erosion pixels were detected within the very-low-susceptibility zone. Conversely, the percentage of erosion pixels progressively increased from the low to the very high susceptibility classes. This pattern confirms the model's effectiveness in accurately identifying and delineating areas based on historical soil erosion patterns.

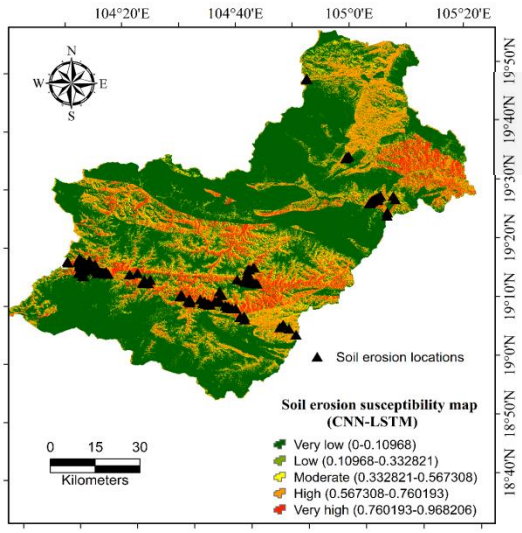



*Figure 7*. Soil erosion susceptibility map produced using the hybrid CNN-LSTM model

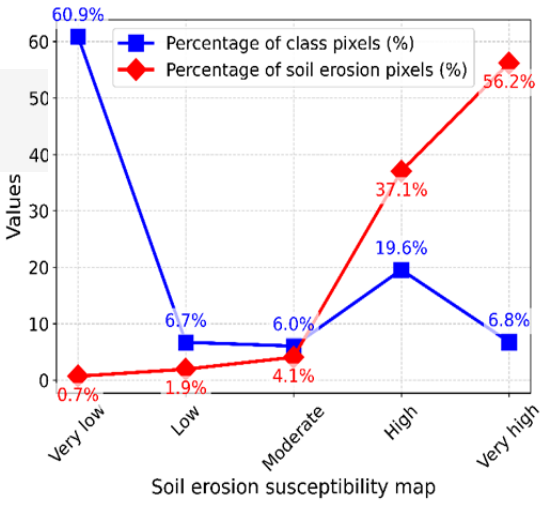



*Figure 8*. Classification analysis of the generated soil erosion susceptibility map

## 6. Discussions

Soil erosion is a temporally and spatially dynamic phenomenon, driven by complex interactions between rainfall patterns, land cover, topography, and human activity. Therefore, effective predictive modeling hinges not only on recognizing spatial heterogeneities but also on understanding temporal dependencies. The comparative analysis of the four DL models revealed significant differences in their ability to address these dimensions.

The CNN-LSTM hybrid model's success lies in its capacity to harness both spatial abstraction and temporal sequencing. CNN layers act as efficient front-end processors that distill multivariate environmental inputs, such as topography, climate, and land use, into compact feature representations. These are then passed to the LSTM layers, which track the evolution of these spatial features (Tahir et al., 2024; Zhang et al., 2024). This architectural synergy reflects the real-world nature of erosion, in which spatial terrain features modulate the impact of temporal drivers such as rainfall or land cover changes (Zha et al., 2022). The hybrid model's strong validation performance and stability indicate an architecture that is both expressive and resilient. Unlike the standalone LSTM, the hybrid model did not overly commit to temporal sequences at the expense of spatial structure. The hybrid model's robustness suggests better regularization and feature disentanglement, enabling it to distinguish persistent patterns from transient fluctuations (Kim and Cho, 2019). This makes the CNN-LSTM particularly valuable in applications where both spatial diversity and time-series consistency are critical. These results align with previous findings that the hybrid CNN-LSTM model is effective in addressing various real-world problems, including the prediction of monthly gas field production (Zha et al., 2022), the seismic response of high-speed railways (Zhang et al., 2024), and soil temperature in diverse large-scale regional climates (Farhangmehr et al., 2025).

The LSTM architecture is inherently suited for sequence modeling (Ewees et al., 2022), which explains its strong ability to capture delayed and cumulative effects of environmental variables, such as seasonal rainfall buildup or progressive vegetation depletion. LSTM recurrent structure allows it to retain memory over long sequences, a critical advantage when modeling soil erosion processes that unfold over time (Su and Kuo, 2022). This temporal acuity likely enabled the LSTM to detect subtle precursors of erosion events, contributing to its high discriminative capacity. However, the same temporal sensitivity can be a liability. The performance dip observed during validation suggests that the LSTM may have overfit to temporal patterns specific to the training set, thereby reducing its generalization to new scenarios. This risk is heightened when training data exhibits periodicity or autocorrelation that does not generalize well. Furthermore, LSTM models are resource-intensive and require careful regularization and sequence engineering to prevent memorization of noise or irrelevant temporal artifacts (Abotaleb and Dutta, 2024).

The DNN's stable performance across both training and validation phases demonstrates a commendable level of generalization, likely due to its simpler structure and reduced risk of overfitting (Mittal, 2020). This consistency makes the DNN an attractive candidate for baseline predictions, especially in operational contexts where model transparency and computational efficiency are priorities. Nonetheless, the DNN's major shortcoming is its lack of temporal context. This model treats all inputs as independent, thereby ignoring causal relationships that unfold over time, such as the delayed onset of erosion following antecedent rainfall events. As a result, DNNs can struggle with time-lagged effects and

cumulative processes, often oversimplifying scenarios that require sequential reasoning. Thus, while DNNs may provide reliable first-level classifications, they fall short in environments where history matters.

CNNs are particularly adept at recognizing localized spatial features, making them effective for processing raster-based inputs, such as elevation maps that encode spatial patterns (Maxwell et al., 2020). This explains the CNN model's reasonable performance in identifying characteristic landforms or vegetation patches associated with erosion-prone areas (Miao et al., 2024). Their hierarchical feature extraction enables them to learn increasingly abstract representations, which help reduce noise and enhance the interpretability of spatial patterns. However, CNNs lack any native mechanism to account for the evolution of these features over time. This architectural limitation becomes a bottleneck in erosion modeling, where the significance of a spatial feature (e.g., a bare slope) may depend heavily on preceding rainfall sequences or seasonal dynamics. Without access to temporal context, CNNs are liable to misclassify temporally nuanced cases, such as delayed erosion events or those mitigated by recent vegetation recovery. Thus, while CNNs remain useful in tasks dominated by spatial structure, their isolated application in time-sensitive problems is inherently constrained.

The comparative performance of these four models highlights a central principle: the alignment of model architecture with domain-specific dynamics is critical. Soil erosion, being both temporally cumulative and spatially heterogeneous, cannot be accurately modeled using architectures that neglect either dimension. LSTM and CNN-LSTM excelled because they embed time-awareness into the learning process. CNN-LSTM, in particular, stood out for maintaining equilibrium between spatial granularity and temporal foresight, making it the most robust and adaptable model in this context. In contrast, while DNNs and CNNs offered computational simplicity and moderate accuracy, their inability to internalize temporal dependencies limits their predictive depth. These models may still be useful in hybrid systems, as pre-classifiers, feature generators, or low-cost alternatives. Still, they are less suited for capturing the full complexity of soil erosion dynamics.

The SHAP analysis highlights geology and elevation as the most influential drivers of soil erosion risk, with both variables showing varying impacts across their specific classes. The dominant influence of these variables on soil erosion risk stems from their fundamental control over soil properties and landscape morphology. Geological formations determine soil texture, cohesion, and erodibility, while elevation influences slope steepness and gravitational forces driving sediment movement (Lakhili et al., 2025). Aspect's notable role reflects its impact on microclimatic conditions, such as sunlight exposure and moisture retention, which affect vegetation cover and runoff patterns (Bhatla et al., 2025). These insights imply that erosion mitigation efforts should focus primarily on stabilizing vulnerable geological substrates and managing topographic features. Strategies such as targeted reforestation, terracing, and land-use planning tailored to elevation and aspect variations are likely to be more effective (Jaafari et al., 2022). Additionally, incorporating detailed geological and topographical data into predictive models can enhance risk assessments and support sustainable land management decisions.

## 7. Concluding remarks

In this study, we applied four deep learning architectures, three standalone models (DNN, CNN, and LSTM) and one hybrid model (CNN-LSTM), to develop a robust framework for soil erosion susceptibility mapping in a representative region of Nghe An province,

Vietnam. The primary goal was to construct a predictive model capable of accurately identifying and mapping erosion-prone areas based on a suite of environmental and topographic variables. Ten key factors known to influence soil erosion were considered: elevation, slope degree, aspect, curvature, NDVI, rainfall, geology, TW, SPI, and soil type. The deep learning models were rigorously evaluated through both training and validation phases using a comprehensive set of performance metrics. Among the tested architectures, the hybrid CNN-LSTM model demonstrated superior generalization capability, achieving the best validation performance for soil erosion prediction. The LSTM model, while excelling during training due to its temporal modeling capabilities, exhibited signs of overfitting, indicating that its sensitivity to sequential patterns may limit generalizability when exposed to unseen data. The DNN model demonstrated consistent, stable performance, making it a reliable, albeit less sophisticated, option. Its lack of temporal modeling capacity limited its ability to capture erosion dynamics fully, but it still proved viable for generalization. The CNN model, while effective at learning spatial patterns, lacked the temporal depth needed for optimal performance, resulting in lower predictive accuracy and discriminative power than other models. To evaluate the relative contribution of these variables, SHAP method was employed. The results highlighted geology, elevation, and aspect as the most influential driving factors, reinforcing the pivotal role of terrain in driving erosion processes and the necessity of incorporating both spatial and environmental heterogeneity in predictive models.

These findings collectively point to the clear advantage of hybrid architectures for environmental modeling tasks involving spatiotemporal complexity. Future work should explore the applicability of the CNN-LSTM model across varied geographic regions and under different climatic and land-use conditions. Incorporating additional data sources, such as time-series satellite imagery or anthropogenic activity indices, alongside seasonal or long-term climatic trends could further enhance model robustness. Continued refinement of such hybrid deep learning frameworks holds significant promise for improving the precision and applicability of soil erosion risk assessments, ultimately supporting more effective land management and conservation strategies worldwide.

## Acknowledgements

We extend our sincere appreciation to the various organizations and agencies that provided us with the data used in this study. This research is funded by the project of the Ministry of Education and Training under grant number B2025-TDV-04.

## References

Abdel-Jaber H., Devassy D., Al Salam A., Hidaytallah L., El-Amir M., 2022. A review of deep learning algorithms and their applications in healthcare. Algorithms, 15(2), 71. https://doi.org/10.3390/a15020071.

Abotaleb M., Dutta P.K., 2024. Optimizing bidirectional long short-term memory networks for univariate time series forecasting: a comprehensive guide. Hybrid Information Systems: Nonlinear Optimization Strategies with Artificial Intelligence, 443. Doi: 10.1515/9783111331133-001.

Adnan R.M., Jaafari A., Mohanavelu A., Kisi O., Elbeltagi A., 2021. Novel ensemble forecasting of streamflow using locally weighted learning algorithm. Sustainability, 13(11), 5877. https://doi.org/10.3390/su13115877.

Archana R., Jeevaraj P.E., 2024. Deep learning models for digital image processing: a review. Artificial Intelligence Review, 57(1), 11. https://doi.org/10.1007/s10462-023-10631-z.

Bag R., Mondal I., Dehbozorgi M., Bank S.P., Das D.N., Bandyopadhyay J., Pham Q.B., Al-Quraishi A.M.F.,

Nguyen X.C., 2022. Modelling and mapping of soil erosion susceptibility using machine learning in a tropical hot sub-humid environment. Journal of Cleaner Production, 364, 132428. https://doi.org/10.1016/j.jclepro.2022.132428.

Bengio Y., Lecun Y., Hinton G., 2021. Deep learning for AI. Communications of the ACM, 64(7), 58−65. https://doi.org/10.1145/3448250.

Bhatla R., Singh R., Kannojiya P.K., 2025. Geospatial mapping of terrain dynamics and rainfall patterns for hazard mitigation in Sikkim. Journal of Earth System Science, 134(1), 1. https://doi.org/10.1007/s12040-024-02464-3.

Bhattacharyya R., Ghosh B.N., Mishra P.K., Mandal B., Rao C.S., Sarkar D., Das K., Anil K.S., Lalitha M., Hati K.M., 2015. Soil degradation in India: Challenges and potential solutions. Sustainability, 7(4), 3528−3570. https://doi.org/10.3390/su7043528.

Chakrabortty R., Ali T., Pal T., Pande C.B., Elaksher A.F., Abioui M., 2026. Climate Change and Land Use Dynamics: Modeling Soil Erosion Scenarios to Achieve Sustainable Development Goals. Earth Systems and Environment, 10(1), 749–774. https://doi.org/10.1007/s41748-025-00631-0.

Chakrabortty R., Pal S.C., Sahana M., Mondal A., Dou J., Pham B.T., Yunus A.P., 2020. Soil erosion potential hotspot zone identification using machine learning and statistical approaches in eastern India. Natural Hazards, 104, 1259−1294. https://doi.org/10.1007/s11069-020-04213-3.

Choubin B., Jaafari A., Henareh J., Karimi O., Sajedi Hosseini F., 2025. Explainable artificial intelligence (XAI) for interpreting predictive models and key variables in flood susceptibility. Results in Engineering, 27, 105976. https://doi.org/10.1016/j.rineng.2025.105976.

Dao D.V., Jaafari A., Bayat M., Mafi-Gholami D., Qi C., Moayedi H., Phong T.V., Ly H.-B., Le T.-T., Trinh P.T., Luu C., Quoc N.K., Thanh B.N., Pham B.T., 2020. A spatially explicit deep learning neural network model for the prediction of landslide susceptibility. CATENA, 188, 104451. https://doi.org/10.1016/j.catena.2019.104451.

Dinh N.C., Manh N.D., Lan N.C., Tuan N.A., Prakash I., Dung V.Q., Kien N.T., Nghia D.T., Van Thang N., 2026. GIS-Based Flow-R Model for Debris Flow Susceptibility Mapping: A Case Study from Muong Bo, Lao Cai, Vietnam. Journal of Science and Transport Technology, 6(1), 29−47. https://doi.org/10.58845/jstt.utt.2026.en.6.1.29-47.

Doan V.L., Nguyen C.C., Nguyen B.Q., Pham L.T., Nguyen T.Q., Trang L.H., 2026. Landslide Susceptibility Mapping under Extreme Events: Evidence from the October 2020 Event in Phuoc Son area, Danang city, Vietnam. Journal of Science and Transport Technology, 6(2), 256−276. https://doi.org/10.58845/jstt.utt.2026.en.6.2.256-276.

Ehteram M., Afshari Nia M., Panahi F., Farrokhi A., 2024. Read-First LSTM model: A new variant of long short term memory neural network for predicting solar radiation data. Energy Conversion and Management, 305, 118267. https://doi.org/10.1016/j.enconman.2024.118267.

Ewees A.A., Al-Qaness M.A.A., Abualigah L., Elaziz M.A., 2022. HBO-LSTM: Optimized long short term memory with heap-based optimizer for wind power forecasting. Energy Conversion and Management, 268, 116022. https://doi.org/10.1016/j.enconman.2022.116022.

Farhangmehr V., Imanian H., Mohammadian A., Cobo J.H., Shirkhani H., Payeur P., 2025. A spatiotemporal CNN-LSTM deep learning model for predicting soil temperature in diverse large-scale regional climates. Science of The Total Environment, 968, 178901. https://doi.org/10.1016/j.scitotenv.2025.178901.

Fathalla A., Li K., Salah A., Mohamed M.F., 2022. An LSTM-based distributed scheme for data transmission reduction of IoT systems. Neurocomputing, 485, 166−180. https://doi.org/10.1016/j.neucom.2021.02.105.

Firoozi A.A., Firoozi A.A., 2025. Introduction to Soil Erosion: Scope, Significance, and Framework. Doi: 10.5772/intechopen.1009419.

Flowers R.M., Ehlers T.A., 2018. Rock erodibility and the interpretation of low-temperature thermochronologic data. Earth and Planetary Science Letters, 482, 312−323. https://doi.org/10.1016/j.epsl.2017.11.018.

Gabbard D., Huang C., Norton L., Steinhardt G., 1998. Landscape position, surface hydraulic gradients and erosion processes. Earth Surface Processes and Landforms: The Journal of the British Geomorphological Group, 23(1), 83−93. https://doi.org/10.1002/(SICI)1096-9837(199801)23:1%3C83::AID-ESP825%3E3.0.CO;2-Q.

Garrido F., Granda P., 2024. Risk Analysis of Soil Erosion Using Remote Sensing, GIS, and Machine Learning Models in Imbabura Province, Ecuador. SN Computer Science, 5(7), 824. https://doi.org/10.1007/s42979-024-03150-3.

Ghasemian B., Shahabi H., Shirzadi A., Al-Ansari N., Jaafari A., Kress V.R., Geertsema M., Renoud S., Ahmad A., 2022. A robust deep-learning model for landslide susceptibility mapping: A case study of Kurdistan Province, Iran. Sensors, 22(4), 1573. https://doi.org/10.3390/s22041573.

Gomiero T., 2016. Soil degradation, land scarcity and food security: Reviewing a complex challenge. Sustainability, 8(3), 281. https://doi.org/10.3390/su8030281.

Hieu T.T., Cham D.D., Van Tien P., Quan N.C., Hai P.T., Anh N.D., Thao B.P., Van T.T.T., Trinh N.Q., Thanh N.T., Cuong T.Q., 2026. Landslide detection and susceptibility analysis: A case study in Pieng stream catchment, Son La province. Journal of Science and Transport Technology, 6(1), 282−299. https://doi.org/10.58845/jstt.utt.2026.en.6.1.282-299.

Hochreiter S., Schmidhuber J., 1997. Long short-term memory. Neural Computation, 9(8), 1735−1780. Doi: 10.1162/neco.1997.9.8.1735.

Huntley B.J., 2023. Solar Energy, Temperature and rainfall. In: Ecology of Angola: Terrestrial Biomes and Ecoregions. Springer, 95−125. https://doi.org/10.1007/978-3-031-18923-4_5.

Istanbulluoglu E., Bras R.L., 2005. Vegetation-modulated landscape evolution: Effects of vegetation on landscape processes, drainage density, and topography. Journal of Geophysical Research: Earth Surface, 110(F2). https://doi.org/10.1029/2004JF000249.

Istanbulluoglu E., Bras R.L., 2006. On the dynamics of soil moisture, vegetation, and erosion: Implications of climate variability and change. Water Resources Research, 42(6). https://doi.org/10.1029/2005WR004113.

Jaafari A., Janizadeh S., Abdo H.G., Mafi-Gholami D., Adeli B., 2022. Understanding land degradation induced by gully erosion from the perspective of different geoenvironmental factors. Journal of Environmental Management, 315, 115181. https://doi.org/10.1016/j.jenvman.2022.115181.

Jaafari A., Najafi A., Rezaeian J., Sattarian A., 2015. Modeling erosion and sediment delivery from unpaved roads in the north mountainous forest of Iran. GEM - International Journal on Geomathematics, 6(2), 343−356. Doi: 10.1007/s13137-014-0062-4.

Jaafari A., Rashidi F., Choubin B., Pham B.T., 2026. An explainable machine learning framework for sustainable land-use planning: A case study of poplar farming suitability. Environmental Impact Assessment Review, 121, 108493. https://doi.org/10.1016/j.eiar.2026.108493.

Janiesch C., Zschech P., Heinrich K., 2021. Machine learning and deep learning. Electronic markets, 31(3), 685−695. https://doi.org/10.1007/s12525-021-00475-2.

Kader Z., Islam M.R., Aziz M.T., Hossain M.M., Islam M.R., Miah M., Jaafar W.Z.W., 2024. GIS and AHP-based flood susceptibility mapping: a case study of Bangladesh. Sustainable Water Resources Management, 10(5), 170. https://doi.org/10.1007/s40899-024-01150-y.

Kennelly P.J., 2008. Terrain maps displaying hill-shading with curvature. Geomorphology, 102(3−4), 567−577. https://doi.org/10.1016/j.geomorph.2008.05.046.

Kim T.-Y., Cho S.-B., 2019. Predicting residential energy consumption using CNN-LSTM neural networks. Energy, 182, 72−81. https://doi.org/10.1016/j.energy.2019.05.230.

Kinnell P., 2005. Raindrop-impact-induced erosion processes and prediction: a review. Hydrological Processes: An International Journal, 19(14), 2815−2844. https://doi.org/10.1002/hyp.5788.

Kopecký M., Macek M., Wild J., 2021. Topographic Wetness Index calculation guidelines based on

measured soil moisture and plant species composition. Science of the Total Environment, 757, 143785. https://doi.org/10.1016/j.scitotenv.2020.143785.

Kumar R., Ha H., Son N.D., Nguyen L.H., 2025. Optimizing CNN, SVM, and MLP for Prediction of Compressive Strength of Concrete using Grid Search Optimization. Journal of Science and Transport Technology, 5(4), 198−217. https://doi.org/10.58845/jstt.utt.2025.en.5.4.198-217.

Kumar R., Tuan N.T., 2026. Landslide Susceptibility Modeling and Mapping: A Comparison of Frequency Ratio and Decision Tree Models. Journal of Science and Transport Technology, 6(2), 315−338. https://doi.org/10.58845/jstt.utt.2026.en.6.2.315-338.

Lakhili F., El Amarty F., Chakir A., Hattafi Y., Fikri N., Benaabidate L., Lahrach A., 2025. Comparative evaluation of machine learning model and PAP/CAR approach for water erosion prediction in the Beht watershed, Morocco. Ecological Engineering & Environmental Technology (EEET), 26(6), 188−204. https://doi.org/10.12912/27197050/203663.

Le Minh N., Truyen P.T., Van Phong T., Jaafari A., Amiri M., Van Duong N., Van Bien N., Duc D.M., Prakash I., Pham B.T., 2023. Ensemble models based on radial basis function network for landslide susceptibility mapping. Environmental Science and Pollution Research, 30(44), 99380−99398. https://doi.org/10.1007/s11356-023-29378-9.

LeCun Y., Bengio Y., Hinton G., 2015. Deep learning. Nature, 521(7553), 436−444. https://doi.org/10.1038/nature14539.

Lundberg S.M., Lee S.-I., 2017. A unified approach to interpreting model predictions. Advances in Neural Information Processing Systems, 30. https://doi.org/10.48550/arXiv.1705.07874.

Ma Z., Mei G., 2021. Deep learning for geological hazards analysis: Data, models, applications, and opportunities. Earth-Science Reviews, 223, 103858. https://doi.org/10.1016/j.earscirev.2021.103858.

Malashin I., Tynchenko V., Gantimurov A., Nelyub V., Borodulin A., 2024. Applications of Long Short-Term Memory (LSTM) Networks in Polymeric Sciences: A Review. Polymers, 16(18), 2607. https://doi.org/10.3390/polym16182607.

Matsuo Y., LeCun Y., Sahani M., Precup D., Silver D., Sugiyama M., Uchibe E., Morimoto J., 2022. Deep learning, reinforcement learning, and world models. Neural Networks, 152, 267−275. https://doi.org/10.1016/j.neunet.2022.03.037.

Maxwell A.E., Odom W.E., Shobe C.M., Doctor D.H., Bester M.S., Ore T., 2023. Exploring the Influence of Input Feature Space on CNN-Based Geomorphic Feature Extraction From Digital Terrain Data. Earth and Space Science, 10(5), e2023EA002845. https://doi.org/10.1029/2023EA002845.

Maxwell A.E., Pourmohammadi P., Poyner J.D., 2020. Mapping the topographic features of mining-related valley fills using mask R-CNN deep learning and digital elevation data. Remote Sensing, 12(3), 547. https://doi.org/10.3390/rs12030547.

Miao S., Liu Y., Liu Z., Shen X., Liu C., Gao W., 2024. A Novel Attention-Based Early Fusion Multi-Modal CNN Approach to Identify Soil Erosion Based on Unmanned Aerial Vehicle. IEEE Access, 12, 95152 –95164. Doi: 10.1109/ACCESS.2024.3425654.

Mienye I.D., Swart T.G., Obaido G., 2024. Recurrent neural networks: A comprehensive review of architectures, variants, and applications. Information, 15(9), 517. https://doi.org/10.3390/info15090517.

Mittal S., 2020. A survey on modeling and improving reliability of DNN algorithms and accelerators. Journal of Systems Architecture, 104, 101689. https://doi.org/10.1016/j.sysarc.2019.101689.

Morgan R.P.C., 2009. Soil erosion and conservation. John Wiley & Sons.

Mosaffaie J., Ekhtesasi M.R., Dastorani M.T., Azimzadeh H.R., Zare Chahuki M.A., 2015. Temporal and spatial variations of the water erosion rate. Arabian journal of Geosciences, 8(8), 5971−5979. https://doi.org/10.1007/s12517-014-1628-z.

Nahib I., Wahyudin Y., Amhar F., Ambarwulan W., Nugroho N.P., Pranoto B., Cahyana D., Ramadhani F., Suwedi N., Darmawan M., 2024. Analysis of Factors Influencing Spatial Distribution of Soil Erosion under Diverse Subwatershed Based on Geospatial Perspective: A Case Study at Citarum Watershed, West Java, Indonesia. Scientifica, 1, 7251691. https://doi.org/10.1155/2024/7251691.

Nguyen T.-H., Le V.-H., Technology T., 2026. Cross-Branch CNN-MLP Integration for Improving Landslide Spatial Probability on Mt. Umyeon, Korea. Journal of Science and Transport Technology, 6(1), 183−198. https://doi.org/10.58845/jstt.utt.2026.en.6.1.183-198.

Nguyen T.G., Tran T.D., Nguyen C.T., 2023. A Optimizing the Long Short-Term Memory (LSTM) model by Bayesian method for salinity intrusion forecasting: a study at Dai Ngai station, Soc Trang province, Vietnam. Vietnam Journal of Marine Science and Technology, 23(3), 223−232. https://doi.org/10.15625/1859-3097/18174.

Nguyen V.-T., Nguyen T.-T., Thi M.N., Hai Y.H., Hong L.V.T., Ngoc D.M., Prakash I., Van Phong T., 2025. Forecasting Deep-Seated Landslide Displacements Using Machine Learning and Automated Monitoring Data. Journal of Science and Transport Technology, 87−106. https://doi.org/10.58845/jstt.utt.2025.en.5.4.87-106.

Nhat V.H., Trinh P.T., Cam L.V., Dieu B.T., Van Hiep L., Prakash I., Anh N.N., Van Hong N., Thanh N.D., Thao N.P., 2025. Mapping Cadmium Contamination Potential in Surface Soil for Civil Engineering Applications: A Comparative Study of Machine Learning and Deep Learning Models in the Gianh River Basin, Vietnam. Journal of Science and Transport Technology, 48−70. https://doi.org/10.58845/jstt.utt.2025.en.5.2.48-70.

Ozbayoglu A.M., Gudelek M.U., Sezer O.B., 2020. Deep learning for financial applications: A survey. Applied Soft Computing, 93, 106384. https://doi.org/10.1016/j.asoc.2020.106384.

Panahi M., Jaafari A., Shirzadi A., Shahabi H., Rahmati O., Omidvar E., Lee S., Tien Bui D., 2021. Deep learning neural networks for spatially explicit prediction of flash flood probability. Geoscience Frontiers, 12(3), 101076. https://doi.org/10.1016/j.gsf.2020.09.007.

Pelletier J.D., Barron-Gafford G.A., Gutiérrez-Jurado H., Hinckley E.L.S., Istanbulluoglu E., McGuire L.A., Niu G.Y., Poulos M.J., Rasmussen C., Richardson P., 2018. Which way do you lean? Using slope aspect variations to understand Critical Zone processes and feedbacks. Earth Surface Processes and Landforms, 43(5), 1133−1154. https://doi.org/10.1002/esp.4306.

Pentsos V., Tragoudas S., Wibbenmeyer J., Khdeer N., 2025. A Hybrid LSTM-Transformer Model for Power Load Forecasting. IEEE Transactions on Smart Grid, 16(3), 2624–2634. Doi: 10.1109/TSG.2025.3535407.

Pham B.T., Jaafari A., Nguyen-Thoi T., Van Phong T., Nguyen H.D., Satyam N., Masroor M., Rehman S., Sajjad H., Sahana M., 2020. Ensemble machine learning models based on Reduced Error Pruning Tree for prediction of rainfall-induced landslides. International Journal of Digital Earth, 14(5), 575−596. https://doi.org/10.1080/17538947.2020.1860145.

Pham G.H., Pham B.T.T., Hoang K.O.T., Tran T.T., Chi H.N.Đ., 2026. GIS Based Soil Erosion Susceptibility Assessment Using Deep Learning Models: A Case Study in the Mountainous Region of Nghe An, Vietnam. Journal of Science and Transport Technology, 67−86. https://doi.org/10.58845/jstt.utt.2026.en.6.1.67-86.

Podhrázská J., Szturc J., Kučera J., Chuchma F., 2025. Impact of Climate Change on Snowmelt Erosion Risk. Land, 14(1), 55. https://doi.org/10.3390/land14010055.

Ramayanti S., Park S., Lee C.-W., Park Y.-C., 2023. High-resolution imaging coupled with deep learning model for classifying water body of Soyang Lake, South Korea. Geosciences Journal, 27(6), 801−813. https://doi.org/10.1007/s12303-023-0032-7.

Razi A., Chen X., Li H., Wang H., Russo B., Chen Y., Yu H., 2023. Deep learning serves traffic safety analysis: A forward-looking review. IET Intelligent Transport Systems, 17(1), 22−71. https://doi.org/10.1049/itr2.12257.

Renard K.G., 1997. Predicting soil erosion by water: a guide to conservation planning with the Revised Universal Soil Loss Equation (RUSLE). US Department of Agriculture, Agricultural Research Service.

Rieke-Zapp D., Nearing M., 2005. Slope shape effects on erosion: a laboratory study. Soil Science Society of America Journal, 69(5), 1463−1471. https://doi.org/10.2136/sssaj2005.0015.

Sarkar T., Mishra M., 2018. Soil erosion susceptibility mapping with the application of logistic regression and artificial neural network. Journal of Geovisualization and Spatial Analysis, 2(1), 8.

https://doi.org/10.1007/s41651-018-0015-9.

Sartori M., Ferrari E., M'Barek R., Philippidis G., Boysen-Urban K., Borrelli P., Montanarella L., Panagos P., 2024. Remaining Loyal to Our Soil: A Prospective Integrated Assessment of Soil Erosion on Global Food Security. Ecological Economics, 219, 108103. https://doi.org/10.1016/j.ecolecon.2023.108103.

Schmidhuber J., 2015. Deep learning in neural networks: An overview. Neural networks, 61, 85−117. https://doi.org/10.1016/j.neunet.2014.09.003.

Singh T., Sharma V., Iltaf S.A., Carrim N.M., 2025. Utilizing LSTM Forecasting and Intelligent Algorithmic Computing for a Dynamic Trading Approach. In: Marketing Intelligence, Part B: AI, Trust, and Innovation in the Modern Business Landscape. Emerald Publishing Limited, 1−21. https://doi.org/10.1108/978-1-83662-560-520251001.

Su Y., Kuo C.-C.J., 2022. Recurrent neural networks and their memory behavior: a survey. APSIPA Transactions on Signal and Information Processing, 11(1). https://doi.org/10.1561/116.00000123.

Tahir M., Ali S., Sohail A., Zhang Y., Jin X., 2024. Unlocking online insights: LSTM exploration and transfer learning prospects. Annals of Data Science, 11(4), 1421−1434. https://doi.org/10.1007/s40745-024-00551-2.

Tarboton D.G., 2003. Rainfall-runoff processes. Utah State University Logan, UT, USA.

Thanh D.Q., Nguyen D.H., Prakash I., Jaafari A., Nguyen V.-T., Van Phong T., Pham B.T., 2020. GIS based frequency ratio method for landslide susceptibility mapping at Da Lat City, Lam Dong province, Vietnam. Vietnam Journal of Earth Sciences, 42(1), 55−66. https://doi.org/10.15625/0866-7187/42/1/14758.

Tran Q.C., Minh D.D., Jaafari A., Al-Ansari N., Minh D.D., Van D.T., Nguyen D.A., Tran T.H., Ho L.S., Nguyen D.H., 2020. Novel ensemble landslide predictive models based on the Hyperpipes Algorithm: A case study in the Nam Dam Commune, Vietnam. Applied Sciences, 10(11), 3710. Doi: 10.3390/app10113710.

Tully K., Sullivan C., Weil R., Sanchez P., 2015. The state of soil degradation in Sub-Saharan Africa: Baselines, trajectories, and solutions. Sustainability, 7(6), 6523−6552. https://doi.org/10.3390/su7066523.

Van Phong T., Trinh P.T., Thanh B.N., Van Hiep L., Pham B.T., 2025. Comparative analysis of machine learning and deep learning methods for coastal erosion susceptibility mapping. Earth Science Informatics, 18(1), 92. https://doi.org/10.1007/s12145-024-01587-x.

Yamashita R., Nishio M., Do R.K.G., Togashi K., 2018. Convolutional neural networks: an overview and application in radiology. Insights into imaging, 9(4), 611−629. https://doi.org/10.1007/s13244-018-0639-9.

Yousefi S., Jaafari A., Valjarević A., Gomez C., Keesstra S., 2022. Vulnerability assessment of road networks to landslide hazards in a dry-mountainous region. Environmental Earth Sciences, 81(22), 521. https://doi.org/10.1007/s12665-022-10650-z.

Yousefi S., Mardanian S., Jaafari A., Tavangar Z., 2026. A reinforcement learning approach with explainable AI for spatial flood susceptibility analysis. Journal of Hydrology: Regional Studies, 63, 103035. https://doi.org/10.1016/j.ejrh.2025.103035.

Zha W., Liu Y., Wan Y, Luo R., Li D., Yang S., Xu Y., 2022. Forecasting monthly gas field production based on the CNN-LSTM model. Energy, 260, 124889. https://doi.org/10.1016/j.energy.2022.124889.

Zhang B., Rong Y., Yong R., Qin D., Li M., Zou G., Pan J., 2022. Deep learning for air pollutant concentration prediction: A review. Atmospheric Environment, 290, 119347. https://doi.org/10.1016/j.atmosenv.2022.119347.

Zhang X., Xie X., Tang S., Zhao H., Shi X., Wang L., Wu H., Xiang P., 2024. High-speed railway seismic response prediction using CNN-LSTM hybrid neural network. Journal of Civil Structural Health Monitoring, 14(5), 1125−1139. https://doi.org/10.1007/s13349-023-00758-6.

Zuazo VcH.D., Pleguezuelo CRoR., 2009. Soil-erosion and runoff prevention by plant covers: a review. Sustainable Agriculture, 785−811. https://doi.org/10.1007/978-90-481-2666-8_48.